GCM Response of Northern Winter Stationary Waves and Storm Tracks to Increasing Amounts of Carbon Dioxide

DAVID B. STEPHENSON

Atmospheric and Oceanic Sciences Program, Princeton University, Princeton, New Jersey

ISAAC M. HELD

Geophysical Fluid Dynamics Laboratory/NOAA, Princeton University, Princeton, New Jersey

(Manuscript received 28 September 1992, in final form 21 April 1993)

ABSTRACT

The response of the Geophysical Fluid Dynamics Laboratory (GFDL) coupled ocean–atmosphere R15, 9-level GCM to gradually increasing CO_2 amounts is analyzed with emphasis on the changes in the stationary waves and storm tracks in the Northern Hemisphere wintertime troposphere. A large part of the change is described by an equivalent-barotropic stationary wave with a high over eastern Canada and a low over southern Alaska. Consistent with this, the Atlantic jet weakens near the North American coast.

Perpetual winter runs of an R15, nine-level atmospheric GCM with sea surface temperature, sea ice thickness, and soil moisture values prescribed from the coupled GCM results are able to reproduce the coupled model's response qualitatively. Consistent with the weakened baroclinicity associated with the stationary wave change, the Atlantic storm track weakens with increasing CO_2 concentrations while the Pacific storm track does not change in strength substantially.

An R15, nine-level atmospheric model linearized about the zonal time-mean state is used to analyze the contributions to the stationary wave response. With mountains, diabatic heating, and transient forcings the linear model gives a stationary wave change in qualitative agreement with the change seen in the coupled and perpetual models. Transients and diabatic heating appear to be the major forcing terms, while changes in zonal-mean basic state and topographic forcing play only a small role. A substantial part of the diabatic response is due to changes in tropical latent heating.

1. Introduction

Many studies have been performed with GCMs in order to investigate the sensitivity of the world climate to increases in carbon dioxide concentration, as summarized in the IPCC (1990) report. While much of the discussion is focused on global mean values, regional changes can be much larger than the global-mean responses and are therefore likely to be more consequential. It is unfortunate that the regional responses in different models differ considerably and it is of utmost importance to understand these differences. The regional responses are dependent upon changes in the circulation of the atmosphere, and it is therefore of use to examine the changes in quantities such as the subtropical jets, the midlatitude storm tracks, and the stationary waves as well as the more often studied surface fields such as surface air temperature and precipitation. Although the circulation in the models differs in significant details from those seen in analyzed observations, it is still a worthwhile exercise to examine the change when GCM parameters are modified, so as to begin to develop the tools needed to understand the sensitivity of the circulation and the associated regional climates.

While many GCM studies have examined the response of surface fields such as surface air temperature to doubled CO_2, a few have also examined the changes in the local jets, stationary waves, and storm tracks. Bates and Meehl (1986) studied the response of blocking frequency in the NCAR (National Center for Atmospheric Research) R15, nine-level doubled CO_2 experiments and found in general a decrease in blocking frequency especially in the Southern Hemisphere. Doubled CO_2 experiments with the NCAR coupled ocean–atmosphere model and the NCAR mixed-layer ocean–atmosphere model were analyzed by Meehl et al. (1993) in order to study the response of ENSO phenomena to increased CO_2. It was found that the midlatitude response to ENSO during winter changed as a result of increased SSTs in the Indonesian region and also due to changes in the basic atmospheric state. The mean wintertime response of the streamfunction in the upper troposphere to the CO_2 change was presented and shows a wave train propagating from the Indone-

Corresponding author address: Dr. David B. Stephenson, Météo-France CNRM/UDC, 42 Ave. G. Coriolis, 31057 Toulouse, France.

sian region around the Pacific rim and down the west coast of North America. In addition, there is a high–low dipole over the North Atlantic with the high centered just south of Greenland and the low centered over the Azores. The response is not dramatic, being of the order of 5×10^6 m^2 s^{-1}, or roughly 20% of the climatological stationary wave values. Siegmund (1990a,b) analyzed the results of the doubled CO_2 experiment performed by Wilson and Mitchell (1987) with the 5° × 7.5° 11-level UKMO GCM. In Siegmund (1990a), the response of the wintertime 500-mb geopotential height field is examined and is found to consist of a complicated pattern with magnitudes of about 70 m. Using a linear stationary wave model it is found that mountains, transients, and diabatic heating all seem to play a part in producing the eddy part[1] of the response. Furthermore, the forcing by diabatic heating is dominated by the latent heating and gives a wave train structure arcing over the Pacific and North America with a low over western North America and a high over eastern North America. The response of the high-frequency transients to doubled CO_2 is examined in Siegmund (1990b) and it is found that the Atlantic storm track, defined by the maximum in the bandpass-filtered 500-mb geopotential height variance, weakens by about 10%. The results of the doubled CO_2 experiment with the higher resolution 2.5° × 3.75° 11-level UKMO GCM[2] have been examined by Hall et al. (1992). The change in the 200-mb streamfunction appears to have a complicated structure not resembling that seen in the aforementioned analyses. The Atlantic storm track shows a weakening in the entrance region of the Atlantic jet.

It is the aim of this paper to investigate the changes in the DJF averaged Northern Hemisphere tropospheric flow of the GFDL coupled ocean–atmosphere GCM as the carbon dioxide concentration is increased gradually. Our interest is in how the stationary waves and storm tracks respond. In order to diagnose the coupled model results we use a perpetual winter atmospheric model prescribing lower boundary conditions from the time-averaged results of the coupled model experiments. The perpetual runs allow us to discover which lower boundary conditions are important in producing the response. The perpetual model also allows us to generate daily data, which is necessary for storm track analysis and was unavailable from the archived monthly mean data of the coupled model. A linear stationary wave model, derived by linearizing the atmospheric GCM about the zonal-mean time-mean basic state, is used to investigate the stationary wave response to increasing carbon dioxide concentrations. Subject to the limitations of this approach, it is possible to find out how the stationary wave response is forced.

2. Numerical Experiments

a. Coupled ocean–atmosphere model

The Geophysical Fluid Dynamics Laboratory (GFDL) Coupled Ocean–Atmosphere Model has been used to investigate the effect of gradually increasing CO_2 concentrations (Stouffer et al. 1989; Manabe et al. 1991; Manabe et al. 1992). The model consists of a nine-level R15 spectral atmosphere model with predicted clouds coupled to a 12-level 3.75° longitude by 4.5° latitude ocean model with a free drift prognostic sea ice model and is described by Gordon and Stern (1982), Bryan and Lewis (1979), and Manabe et al. (1991). Three 100-year integrations were performed by Manabe et al. having 1%, 0, and −1% compounded annual rates of change of carbon dioxide concentration and are known as the *G*, *S*, and *D* integrations, respectively, with the data archived in the form of monthly mean averages. The data was kindly made available to us for the analysis presented in this paper.

As a preview of the results we present the 500-mb eddy geopotential height response and use it to briefly discuss the problem of statistical significance. The *G*-*S* difference in the 500-mb eddy geopotential height averaged over 0–100 years of DJF winters is shown in Fig. 1. Note the wave train–like response with a high over eastern Canada and a low over southern Alaska. While it is not the primary purpose of this paper to enter into a comprehensive statistical analysis of the GCM response, because of the existence of natural climatic variability it is important to ask whether the response is significant and whether the response is representative of the change throughout the 100-year period.

One simple way of estimating significance is by the univariate test described by Chervin and Schneider (1976). The *G*-*S* wave train response in the 500-mb

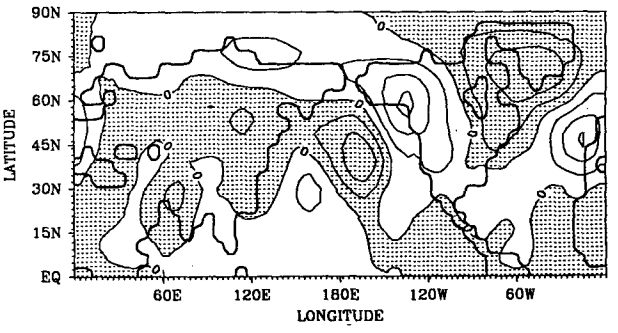

FIG. 1. The 500-mb eddy geopotential height response to increased CO_2 averaged over the 100 years of DJF winters for experiments *G*-*S*. Contour interval of 5 m and shading above zero.

[1] In this paper, an eddy is defined to be a deviation from the zonal mean.

[2] Performed by C. A. Senior and J. F. B. Mitchell and described in the IPCC Report (1990).

eddy geopotential height field is of the order of 40 m in the years 90–100. This can be compared to the standard deviation of the geopotential height at 500 mb taken over the ten decadal means of S or G, which gives typical values of 15 m. Applying Student's t-test gives a t statistic of 2.4, which is 95% significant. This, however, is the case for only the last decade of the G-S response where one expects the response might be the greatest since the carbon dioxide concentration difference is the greatest. For the earlier decades, with smaller differences between G and S, one expects the geopotential height response to become less significant. In Lanzante (1991), the question of significance is studied in more detail and it is found that the signal in Northern Hemisphere winter is just emerging clearly from the natural variability in the latter part of the 100-year run. Knutson (1992, personal communication) has examined an extension of the increasing CO_2 integration up to 180 years, and finds that a similar pattern stands out clearly after year 100. Both the anomalous high and low over Greenland and North America persist with the east coast high becoming the more dominant feature at later times.

The other question is whether the 0–100-year time-mean response is representative of the 100-year period. It is possible that as the CO_2 concentration is increased, the geopotential height response G-S will vary spatially as well as in amplitude. By examination of decadal DJF averages throughout the 100 years, it appeared that any time dependence in the shape of the response was masked by interdecadal natural variability. By performing a linear regression of the height field in the G run with time at each grid point we can obtain an idea of the trend in the G experiment. Fig. 2 shows the eddy part of the regression slope of the 500-mb geopotential height using 20 samples of five-year DJF means. The Pearson product moment correlation coefficient is typically greater than 0.6 at most grid points, which implies that the regression slope is 95% significant using a one-tail Student's t-test. The slope in Fig. 2 has a similar pattern to the mean in Fig. 1.

In what follows, we will take the G-S response to be the DJF mean over the last decade in G minus the DJF mean over the hundred years in S. The 90–100-year decade of G has an increase by a factor of roughly 2.5 in carbon dioxide concentration over that in S. This has the merit that it gives us the strongest and therefore most significant response and hopefully therefore the cleanest signal. The preceding discussion has attempted to justify why we think this is representative of the change due to increasing carbon dioxide concentrations.

b. *Perpetual winter atmosphere model*

The atmospheric response to increased CO_2 can be thought of as partly due to the direct effect of the CO_2 on radiative heating/cooling rates and partly due to the indirect effect through changes in the lower boundary fields on the earth's surface such as sea surface temperatures and sea ice thicknesses. It is of interest to know which lower boundary fields cause the largest tropospheric response. For example, What is the relative importance of the altered sea ice distribution on the atmosphere? To address these questions we performed four runs with a perpetual DJF winter atmosphere model having lower boundary fields prescribed from the time-averaged results of the coupled GCM experiments described in the previous section. The atmosphere model that we used was identical to the nine-level R15 model used in the coupled ocean–atmosphere runs. We decided to prescribe sea surface temperatures, sea ice thicknesses, and soil moisture in the runs and took these values from DJF time averages of the coupled model runs. Soil moisture was prescribed because of the possibility of excessive drying and heating of summer hemisphere continents in perpetual runs; however, soil moisture plays a very minor role in wintertime climates, which we focus on here. The snow cover was not prescribed but was allowed to change throughout the runs. The experiments were forced with DJF average insolation and were run for 3300 days with time averages performed over the last 3000 days. The control run, C, used boundary conditions taken from the 100-year time-mean of the S run. Run A used SSTs and soil moistures from the time mean of the last decade of experiment G, and used the same sea ice thicknesses as used in the control C. Run B used SSTs, soil moistures, and sea ice thicknesses from the time mean of the last decade of experiment G. Finally, we did a run BX that was the same as B except that the CO_2 concentration was increased to 2.5 times the present-day CO_2 value used in the other runs.

The small difference between B and BX confirmed the importance of changes in the lower boundary conditions compared to the direct effect of CO_2 in forcing the troposphere. For both the zonal winds and the stationary waves, it was found that the difference of B and BX runs was less than that of the variability of the runs; hence, the prescribed boundary conditions are

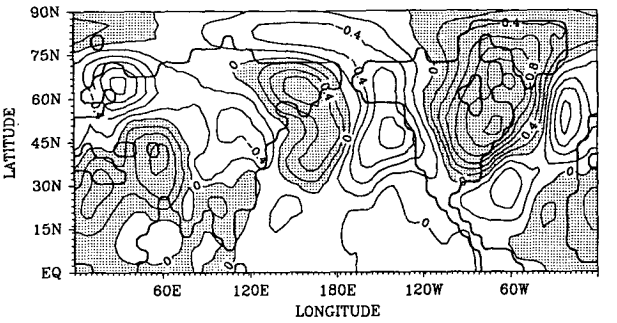

FIG. 2. The eddy part of the linear trend in the 500-mb geopotential height field in experiment G. Contour interval of 0.2 m (5 yr)$^{-1}$ and shading above zero.

the most important factor in the perpetual runs. The direct effect is expected to play a larger role in the middle atmosphere further from the influence of the lower boundary. Henceforth, we shall only discuss the results of the *A*, *B*, and *C* runs and in particular the differences *A-C* and *B-C*. Here *A-C* is the perpetual atmosphere response to changing SSTs and soil moisture, whereas *B-C* is the perpetual response to changing SSTs, soil moisture, and sea ice thicknesses. The difference between responses *A-C* and *B-C* shows the effect that the change in sea ice has upon the atmosphere.

The SSTs and sea ice thicknesses from experiments *S* and *G* are shown in Figs. 3a and 3b and were the ones used for the perpetual winter runs. The difference in SSTs (*G-S*) is shown in Fig. 3c. Note that the SST difference has a complex structure in the North Atlantic with the region south of Greenland actually cooling slightly with increased CO_2 concentration. This is a consequence of deep overturning in the ocean model as described in Manabe et al. (1991). A large amount of sea ice disappears as the CO_2 is increased and it retreats completely from over the Hudson Bay (Manabe et al. 1992). It is of interest to know how significant sea ice change is in regional climate change compared to the effect due to changes in the SSTs.

3. Results

In this section, the responses from the coupled and perpetual runs will be presented and discussed. Each quantity of interest will be presented as differences *G-S*, *A-C*, and *B-C*. Difference *G-S* is the difference between the DJF time mean over the last decade of the *G* run and the DJF time mean over the 100 years of the *S* run, and represents the response of the coupled ocean–atmosphere model to increasing carbon dioxide over years 90–100 of the transient increase. Differences *A-C* and *B-C* are the perpetual atmosphere response to changed lower boundary conditions as described in the previous section. It is of interest to see how well the perpetual model responses *A-C* and *B-C* emulate the coupled model response *G-S*.

Figure 4 shows the surface air temperature response in the three cases. In the coupled model response, note the large increases in the higher latitudes and over North America. Response *B-C* reproduces this whereas response *A-C* fails to do so, indicating that sea ice changes are necessary in reproducing this effect as shown by Ingram et al. (1989). The large increases over North America can be seen in a number of GCM runs with increasing carbon dioxide concentrations [cf. p. 165 of the IPCC (1990) report]. Both *A-C* and *B-C* reproduce the relatively large increases over North America, indicating that the disappearance of sea ice is not the only factor in causing this phenomenon. The perpetual runs with SST and sea ice boundary conditions taken from the coupled model appear to be able to emulate the coupled model response to increased CO_2 in so far as surface air temperatures are concerned.

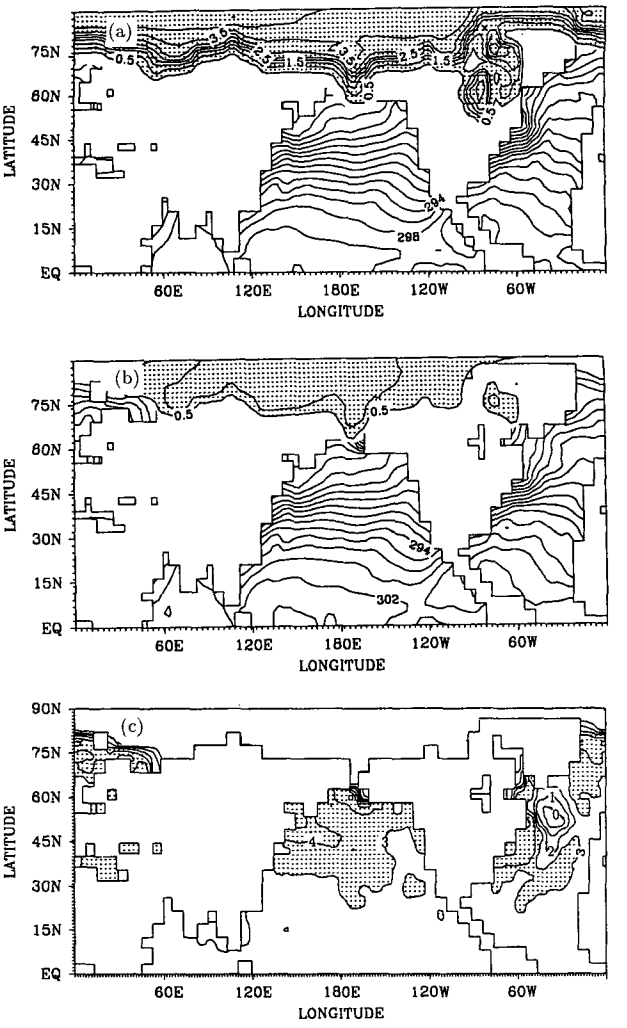

FIG. 3. Sea surface temperatures (*K*) and sea ice thicknesses (*m*) from the coupled model experiments *S* and *G*. (a) SST and sea ice thicknesses averaged over DJF from years 0–100 of the *S* experiment. (b) SST and sea ice thicknesses averaged over DJF from years 90–100 of the *G* experiment. (c) The difference in SSTs *G-S* with a contour interval of 1 K and shading for values exceeding 3 K.

Figure 5 shows the zonal-mean zonal wind responses. All three cases show weakening of the equatorward and strengthening of the poleward flanks of the subtropical jets by amounts less than 5 m s^{-1}. The same decrease in westerlies on the equatorward flanks of the jets occur in the UKMO doubled CO_2 run as is shown in Fig. 14 of Wilson and Mitchell (1987) and in the NCAR model (Washington and Meehl 1989). At high latitudes greater than about 70°, the zonal-mean zonal wind becomes less westerly, especially at upper levels. The upper-level tropical easterlies show a decrease in all three responses. Although we do not focus on the Southern Hemisphere here, it is interesting to note that all three responses show an increase in surface westerlies at 55°S. Perpetual winter atmosphere models forced

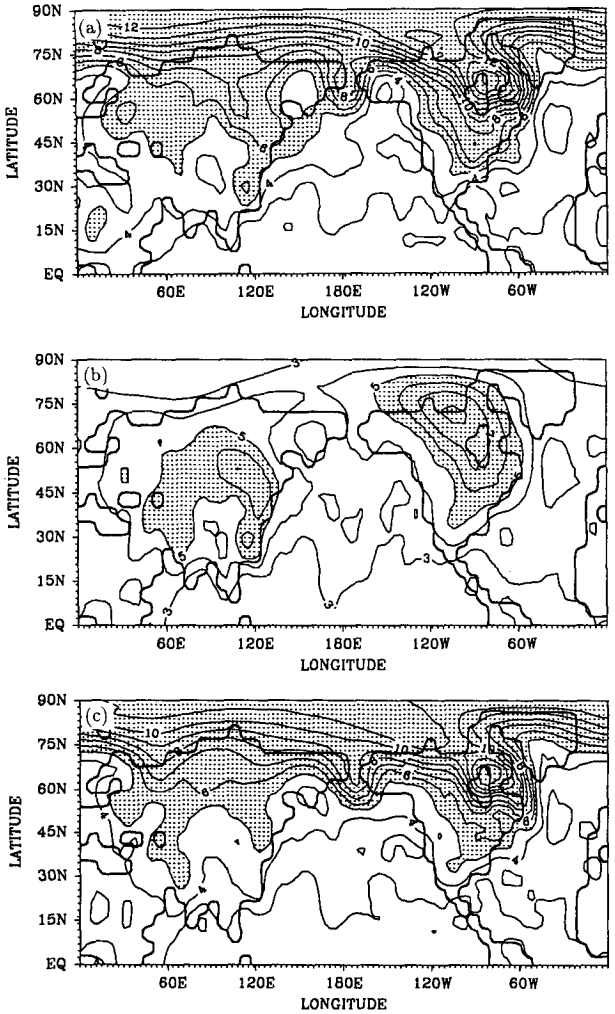

FIG. 4. Surface air temperature responses with a contour interval of 1 K and shading for values greater than 5 K. (a) Coupled run *G-S*. (b) Perpetual run with SST change *A-C*. (c) Perpetual run with both SST and sea ice change *B-C*.

with the appropriate lower boundary conditions can emulate the response of the zonal-mean zonal winds in a coupled ocean–atmosphere model, at least qualitatively.

Figure 6 shows the zonal wind responses at 200 mb. All three responses show a weakening in the entrance region of the Atlantic jet and an intensification in the central Pacific at 45°N. The changes are not large compared to the typical values of 50 m s^{-1} of the westerly jets, being generally less than 5 m s^{-1}. Note that the changes are not very zonally symmetric in that variations around latitude circles are of the same size as the zonal-mean responses. There is a change in the stationary waves in the atmosphere comparable to that seen in the zonal-mean quantities.

Figure 7 shows the responses of the eddy part of the 500-mb geopotential height field. The wave train structure seen in Fig. 1 is even more clearly revealed in the *G-S* response shown in Fig. 7a because of the stronger signal in years 90–100 than in the 100-year averages. Both the perpetual responses also show this structure with the *A-C* case being the closest to that of *G-S*. The response is largest over Baffin Bay and southern Alaska with amplitudes of over 40 m. The response is such that there is less advection of cold northern air over North America, which is consistent with the increased warming noted over the region. It is of interest that the perpetual model response to the SST change alone (*A-C*) provides a better simulation of the coupled model's stationary wave response than does the perpetual model's response to both SST and sea ice changes (*B-C*). We assume that soil moisture is of negligible importance to the climatology of Northern Hemisphere winter. We take this as a warning to focus on only the general structure in Fig. 7 and not on the details. Inspection of the vertical structure of the geo-

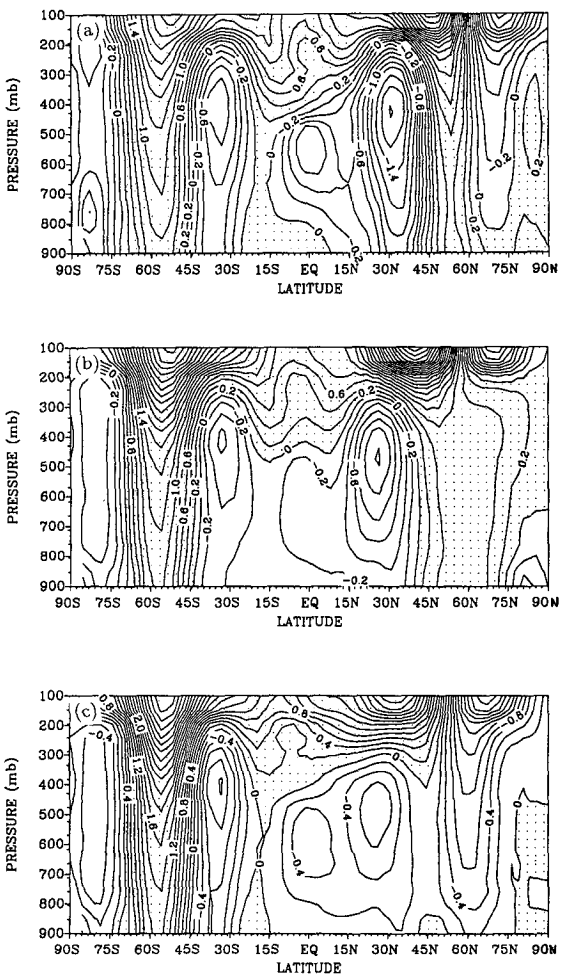

FIG. 5. Zonal-mean zonal wind responses with a contour interval of 0.2 m s^{-1} and shading for values greater than zero. (a) Coupled run *G-S*. (b) Perpetual run with SST change *A-C*. (c) Perpetual run with both SST and sea ice change *B-C*.

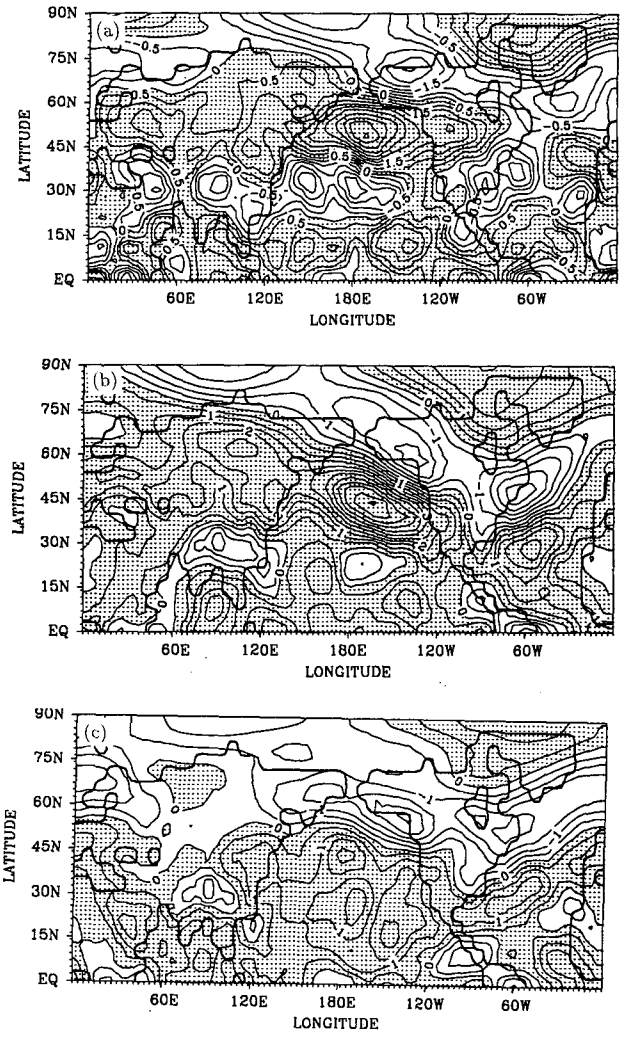

FIG. 6. The 200-mb zonal wind responses with a contour interval of 0.5 m s^{-1} and shading for values greater than zero. (a) Coupled run *G-S*. (b) Perpetual run with SST change *A-C*. (c) Perpetual run with both SST and sea ice change *B-C*.

potential response has shown it to be equivalent barotropic, with largest amplitude at the tropopause. Figure 8 shows the *G-S* response of the 200-mb geopotential height field and it can be seen that the spatial pattern overlays that of Fig. 7a. The similarity of this response to the structure of external Rossby waves suggests that linear stationary wave theory might be used to find the source of the wave train (Held 1983). It is tempting to perceive the wave train as emanating from the tropics; however, the use of a linear stationary wave model leads to the emergence of a far more complicated scenario involving forcing by transients as will be revealed in the next section.

Since the stationary waves have changed with increasing CO_2, it is interesting to speculate on whether there is a corresponding change in the transients. North America has warmed with increasing carbon dioxide concentrations more than the North Atlantic and, hence, the land–sea temperature gradient has decreased on the eastern seaboard where the Atlantic storms intensify. From this argument we would expect a weakened Atlantic storm track due to the reduction in baroclinicity. To define the model storm tracks we use the 2.5–6-day bandpass filtering method pioneered by Blackmon (1976) and described completely in Blackmon et al. (1977). This requires daily data that was not available for the coupled model results, which were archived as monthly means; however, the perpetual model provided us with daily information sufficient to derive storm track statistics. While we are confident that the perpetual model provides reliable simulations of the coupled model's storm tracks, further calculations will be needed for verification. A more important caveat is that the model only has R15 resolution, which

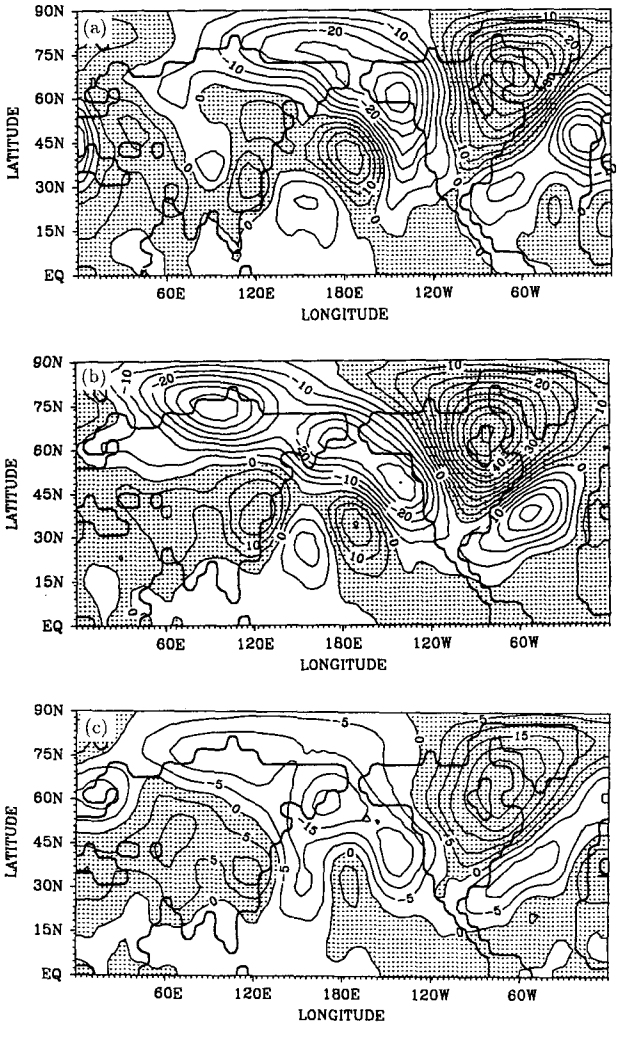

FIG. 7. The 500-mb eddy geopotential height responses with a contour interval of 5 m and shading for values greater than zero. (a) Coupled run *G-S*. (b) Perpetual run with SST change *A-C*. (c) Perpetual run with both SST and sea ice change *B-C*.

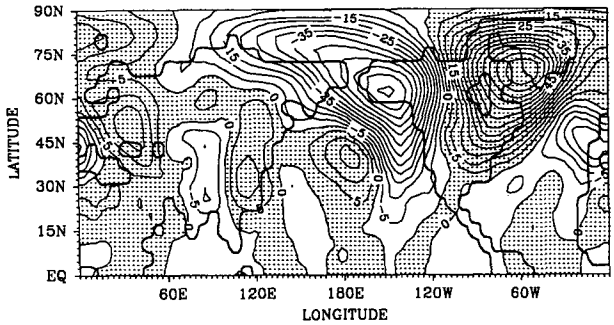

FIG. 8. The 200-mb eddy geopotential height response *G-S* with a contour interval of 5 m and shading for values greater than zero.

is marginal for resolving the synoptic storm activity. Because both the transient heat flux at 800 mb and the rms of the 500-mb geopotential height field give narrowly defined maxima meridionally when defined using 2.5–6-day bandpassed transients we will use these to define the Pacific and Atlantic storm tracks.

Figure 9a shows the rms 500-mb geopotential height field for run *C* of the perpetual model corresponding to present-day values of carbon dioxide. Compared to the observational analysis of ECMWF data presented in Schubert et al. (1990), the model storm tracks are roughly 10% stronger and the maximum in the model Pacific storm track is about 60° east of that in the observed data. The excessive strength of the Pacific storm track in the eastern Pacific is a fairly common problem in atmospheric models and is seen in the high resolution ECMWF models (Klinker 1992, personal communication). Figures 9b and 9c show the changes in this field for perpetual runs *A* and *B*. Run *A-C* shows a decrease of around 5 m in the rms geopotential height in the vicinity of the Atlantic storm track and there is an overall increase in the 45°–60°N latitude band. Run *B-C* shows the same reduction in the Atlantic storm track as in case *A-C* but has weaker reduction elsewhere. Both *A* and *B* runs show an overall decrease in variance in the higher latitudes north of 70°N.

Figure 10a shows the 800-mb sensible poleward heat flux $\overline{v'T'}$ due to transient 2.5–6-day eddies for run *A* of the perpetual model. Compared to observed values in Schubert et al. (1990), the model is about 1.5 times as strong and the Pacific storm track is too far eastward. Figures 9b and 9c show the responses *B-C* and *A-C*, which both display a decrease of roughly 3 K m s^{-1} in the Atlantic storm track. The changes elsewhere are also consistent with the changes in the rms geopotential height shown in Fig. 8b and 8c.

To summarize, the perpetual runs indicate a weakening of the Atlantic storm track with increased CO_2. There is a strengthening of the zonal-mean storminess in the latitude band 45°–60°N in the case where the SSTs are allowed to change but where the sea ice thickness is kept fixed. However, when the sea ice is also changed, this strengthening disappears. The weakening of the Atlantic storm track is consistent with the reduction in baroclinicity expected in this region and with the reduction in the upper-level jet shown in Fig. 6. The weakening of the Atlantic jet in its entrance region is seen in the NCAR results and in both the low- and high-resolution U.K. Meteorological Office (UKMO) results. Furthermore, the weakening of the Atlantic storm track in this region is seen in both the low- and high-resolution UKMO results. The higher-resolution UKMO results show a strengthening of the Atlantic storm track to the northeast of this region (Hall et al. 1992).

4. Linear analysis

Can this change in the stationary wave be modeled by linear stationary wave theory? If so, which are the

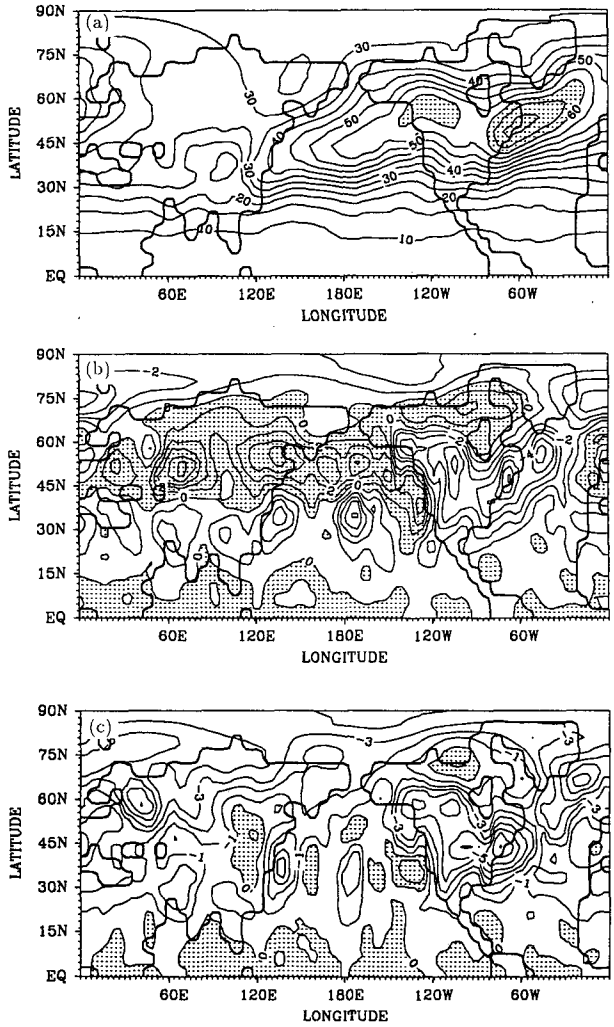

FIG. 9. The 2.5–6-day bandpass filtered 500-mb rms geopotential height for control and responses. (a) Control value in experiment *C* with a contour interval of 5 m and shading for values exceeding 60 m. (b) The response when sea ice is unchanged *A-C* with a contour interval of 1 m and shading for values exceeding zero. (c) The response when sea ice is changed *B-C* with a contour interval of 1 m and shading for values exceeding zero.

most important forcing mechanisms according to the linear model: diabatic heating in the tropics or midlatitudes, orography, transient eddies, or changes in the basic zonal flow? To address these questions we have used a linear stationary wave model forced by the time-averaged results of both the coupled and perpetual GCMs. We linearize about the zonal-mean flow in this paper. Comparable calculations in models linearized about the zonally asymmetric climatological flow will eventually be of interest, but such models result in a more singular matrix to be inverted, and we have chosen to start with the simpler zonally symmetric basic state.

a. *The linear model*

Linear stationary wave models have been developed by a number of groups and have proved useful in diagnosing the results of atmospheric GCMs (Kok et al. 1987; Nigam et al. 1986a,b). A linear model has been constructed that is consistent with the GFDL R15, nine-level atmospheric GCM (Ting and Held 1990). For a discussion of how well the linear model describes the Northern Hemisphere wintertime stationary waves in the GCM, refer to Nigam et al. (1986b) in which a very similar model is used. The model can be forced by orography, diabatic heating, and transients. The diabatic heating is saved from the GCM at each grid point. The transient forcings are deduced as residuals from the time means of the vorticity, divergence, and temperature tendency equations and are known, respectively, as the vorticity transients, the divergence transients, and the temperature transients.

It is necessary to introduce extra damping into the linear model in order to obtain realistic results. The damping can be thought of as acting to mimic the nonlinear cascades that occur in the full GCM especially in the vicinity of critical latitudes. The results from the linear model look very unrealistic if the damping is too small but converge to more realistic patterns for larger values of the damping. The linear model includes subgrid-scale diffusion, low-level Newtonian thermal damping, and low-level Rayleigh friction. The diffusion was set to ∇^4 diffusion with a coefficient of 10^{17} m^4 s^{-1}, ten times the value used in the full GCM, and was applied to the vorticity, divergence, and temperature equations. The Newtonian thermal damping was set to five-day damping below $\sigma = 0.83$, the lowest three levels of the model, and there was no damping at higher levels. The Rayleigh friction was given a damping coefficient of the form $\kappa(\sigma - 0.8)$ for σ below 0.8 and was zero above; the drag constant κ took the value of 0.2 per day. No extra critical-layer damping was included; the ∇^4 diffusion was evidently sufficient to prevent singular behavior at critical latitudes.

The linear model used the forcings and basic states from both the coupled ocean–atmosphere GCM and the perpetual GCM experiments. In the following section we will refer to the linear models by the letter denoting the GCM experiment that was used to provide both the zonal-mean basic state and the forcings.

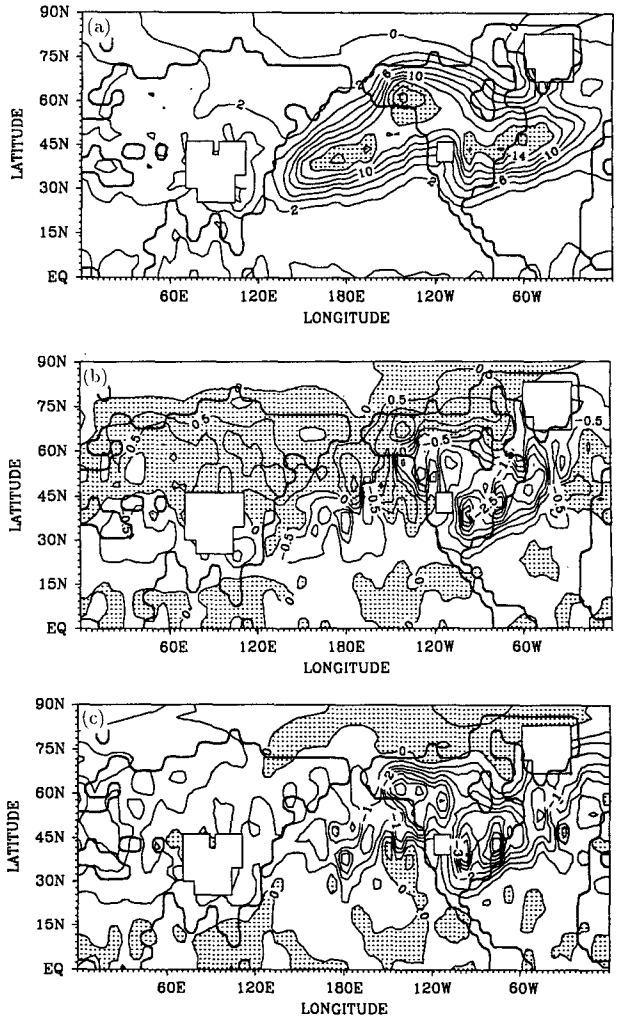

FIG. 10. The 2.5–6-day bandpass filtered 800-mb transient sensible heat flux for control and responses. (a) Control value in experiment *C* with a contour interval of 2 m K s^{-1} and shading for values exceeding 14 m K s^{-1}. (b) The response when sea ice is unchanged *A*-*C* with a contour interval of 0.5 m K s^{-1} and shading for values exceeding zero. (c) The response when sea ice is changed *B*-*C* with a contour interval of 0.5 m K s^{-1} and shading for values exceeding zero.

b. *Linear model results*

Figure 11 shows the linear model results for the 500-mb eddy geopotential height response due to increased CO_2 obtained by forcing the linear model with the coupled and perpetual GCM results. The large-scale features in these figures resemble the GCM response in Fig. 7. In addition, the linear model appears to be reproducing the response of both the coupled and perpetual GCMs, which suggests the linear result is fairly

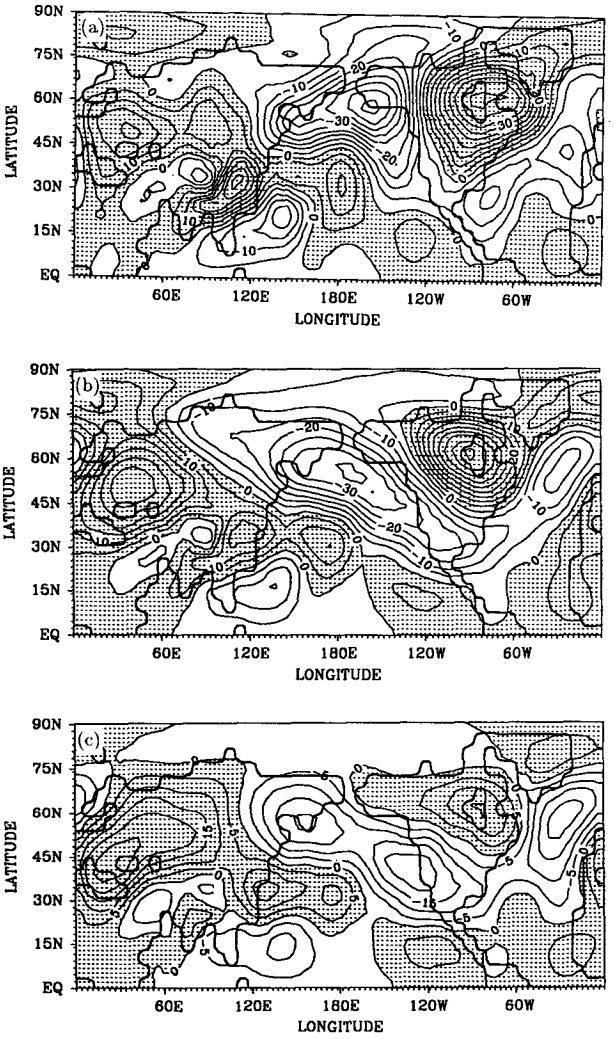

FIG. 11. The 500-mb eddy geopotential height responses of the linear model when forced with all the forcings. Contour interval is 5 m and shading is for values exceeding zero: (a) *G-S*, (b) *A-C*, (c) *B-C*.

robust. In what follows, only the linear model results for the *G-S* case will be presented even though we also performed all the linear model analyses on *A-C* and *B-C*. The linear analysis of the perpetual GCM results gave qualitatively similar results to those shown in the coupled GCM case *G-S*.

It is of interest to see how important each type of forcing is to the total response shown in Fig. 7a. Figures 12a,b,c show the responses *G-S* of the linear model when forced by orography, diabatic heating, and transients. It was decided to only include thermal and vorticity transients and neglect the small effect due to divergence transients. The mountain response is due to weakened westerlies over Tibet and Greenland forcing stationary Rossby waves. The orographic forcing appears to play less of a role than the other forcings but it should be remembered that this balance is sensitive to the low-level winds in the GCM, which are liable to differ from those of the observed climatology (Held and Ting 1990). This also probably accounts for why Siegmund (1990a) deduced that mountains were a major forcing for the stationary wave response in the UKMO model results. The diabatic and transient responses shown in Figs. 12b and 12c both appear to contribute significant amounts to the total response due to changes in the forcings rather than in changes in the zonal-mean basic state. This cause was shown by running the linear model with the same basic state but with the different forcings, which gave very similar results to those presented in Fig. 12b,c.

Figure 13a shows the linear model response to latent heating forcing in the latitude band 20°S to 20°N. By comparison with Fig. 12b, it can be seen that this ex-

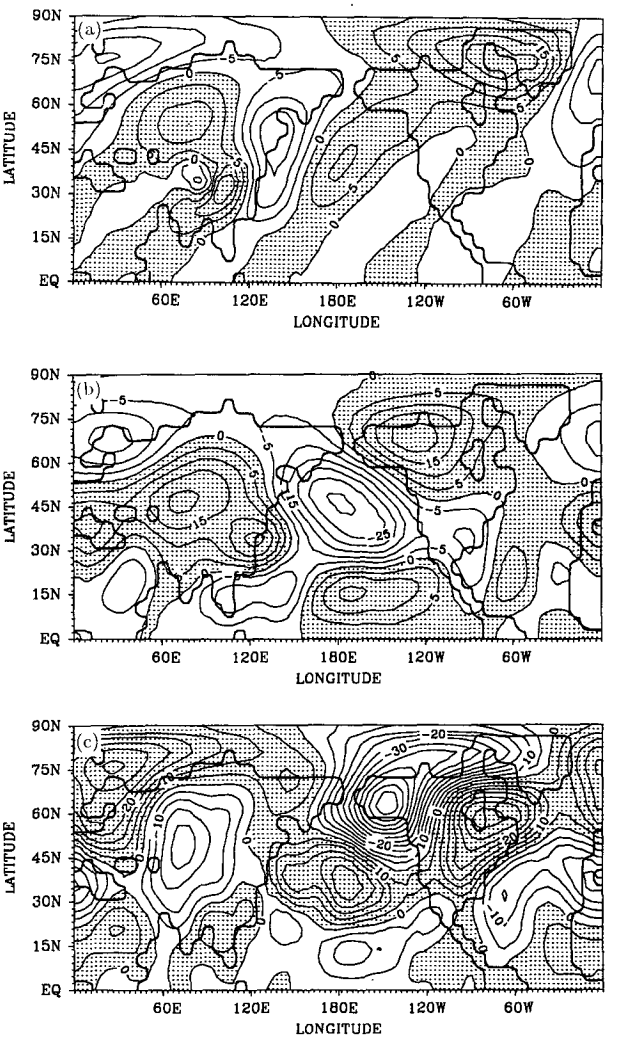

FIG. 12. The 500-mb eddy geopotential height responses (*G-S*) of the linear model when forced with *G* and *S* forcings. Contour interval is 5 m and shading is for values exceeding zero. (a) Mountain forcing. (b) Diabatic forcing. (c) Transient forcing.

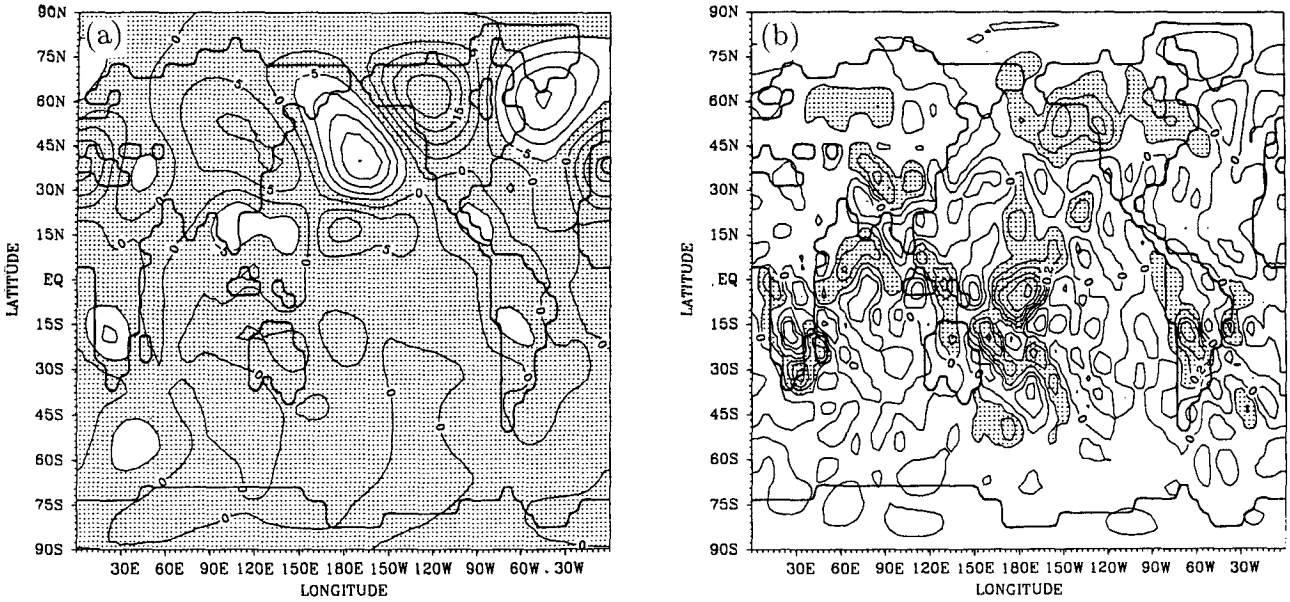

FIG. 13. (a) The 500-mb eddy geopotential height response (G-S) of the linear model to forcing by latent heating in the tropics (20°S–20°N) with a contour interval of 5 m and shading for values greater than zero. (b) Vertically integrated latent heating change G-S with a contour interval of 0.1 K day^{-1} and shading for values exceeding 0.1 K day^{-1}.

plains a significant part of the response to diabatic heating. The latent heating near the date line increases with increasing CO_2 as is shown in Fig. 13b, which depicts the change in vertically integrated latent heating for G-S. The response of the linear model to the tropical latent heating appears to be a Rossby wave propagating out of the tropical Pacific. The heating in the Indonesian region has shifted eastward on average. It is of interest, that a wave train emanating from the tropical Pacific can also be seen in the upper-level streamfunction response in the doubled CO_2 experiments with the NCAR GCM as shown in Fig. 10 of Meehl et al. (1993); it should also be noted that there are marked differences between the GFDL and NCAR wave trains.

The transients play a major role in the response and so it makes sense to examine them in more detail. Figure 14a shows the linear response only to forcing by transients in the temperature equation. There is evidence of the wave train pattern seen in the total G-S GCM response. The same pattern is also seen in Fig. 14b, which shows the inverse Laplacian of the vertically integrated temperature forcing by transients. Comparison to Fig. 14c, which depicts the change G-S in 800-mb eddy temperature with increased CO_2, suggests that the thermal transients are acting similar to $\kappa\nabla^2 T$ damping of the eddy temperature change T with a value of κ of the order of 10^6 m^2 s^{-1}. Rather than forcing the stationary wave response, the thermal transients are responding to it by acting so as to dampen the temperature changes. Figure 15 shows the 500-mb eddy geopotential height response due to forcing by vorticity transients from the coupled runs G-S. Comparison with Fig. 14a indicates that the vorticity transients play at least as large a role as thermal transients in determining the stationary wave response. Furthermore, the pattern is hard to interpret and no simple relationship could be found for the change seen in the vorticity or streamfunction tendency due to the transients. It is possible that R15 may be too low a resolution from which to obtain a reliable signal from the vorticity transients and it would be of interest to repeat the perpetual runs with models having higher spatial resolutions.

5. Discussion

The analysis of the Northern Hemisphere wintertime tropospheric circulation in the GFDL coupled ocean–atmosphere GCM experiments with gradually increasing CO_2 has revealed no dramatic changes but rather changes of the order of 10% at years 90–100 that correspond to an increase in CO_2 concentration by a factor of 2.5. The perpetual winter atmospheric model using prescribed SSTs, sea ice thicknesses, and soil moisture taken from the time-averaged results of the coupled runs seems able to reproduce the response of the coupled model to increased CO_2. We believe that the perpetual model will play an important role in interpreting the results from seasonal coupled GCMs. For example, we could use it to explore further the relative importance of the Atlantic and Pacific SST changes for the circulation over North America.

The linear stationary wave model was able to reproduce the changes seen in the GCM runs at least qualitatively. The dominant forcings are latent heating and

transients with changes in the zonal-mean basic state playing only a minor role. The thermal transients act in a manner so as to diffuse away the stationary wave temperature change. The vorticity transients forced the stationary wave response significantly. Since the linear model analysis suggests that a large part of the stationary wave response is being forced by the change in transients, it is possible that the stationary wave response, and hence a large part of the tropospheric response, will differ in doubled CO_2 experiments performed at higher spatial resolution where it is known that the transients differ considerably from those at lower resolution. The linear analysis also indicates that changes in latent heating in the tropics contribute large amounts to the stationary wave response. It is not clear whether the Atlantic storm track transients are responding to changes in the local low-level thermal gradients or whether they are being partially triggered by the wave train emanating from the tropics. It is clear that the analysis of the tropospheric response to doubled CO_2 in future GCM experiments is a matter of great interest and will hopefully shed some light on the nature of the mutual interaction of atmospheric transient and stationary eddies.

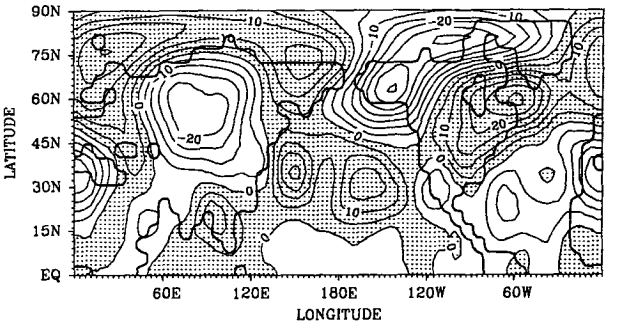

FIG. 15. The 500-mb eddy geopotential height response (*G-S*) of the linear model to forcing by vorticity transients. Contour interval is 5 m and shading is for values greater than zero.

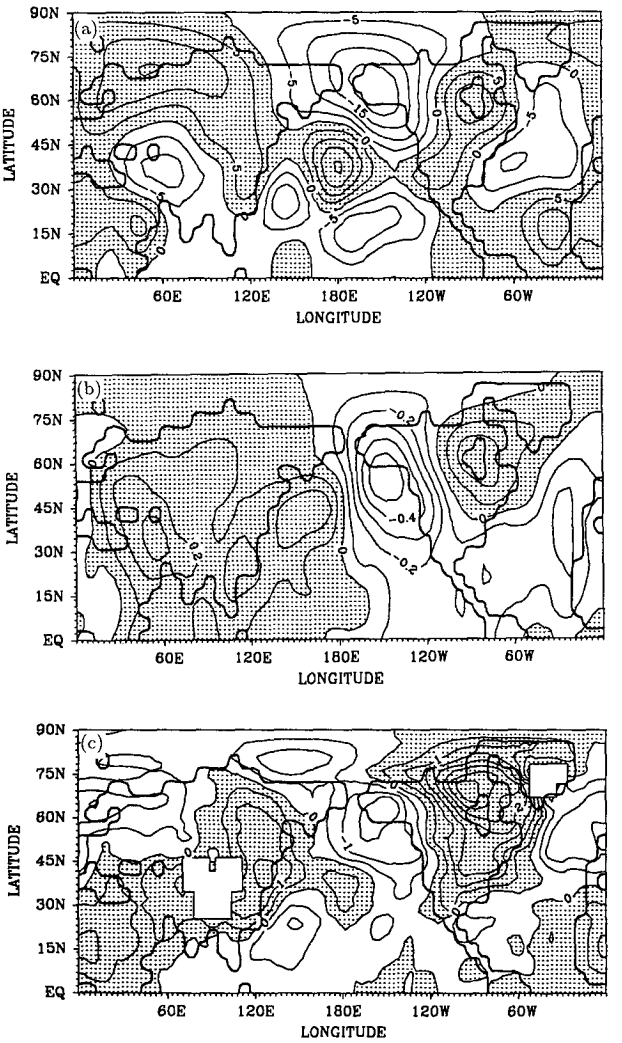

FIG. 14. (a) The 500-mb eddy geopotential height response (*G-S*) of the linear model to forcing by thermal transients with a contour interval of 5 m and shading for values greater than zero. (b) Inverse Laplacian of the vertically integrated thermal transient forcing. (c) The 800-mb eddy temperature response *G-S* with a contour interval of 0.5 K and shading for values exceeding zero.

Acknowledgments. We wish to thank M. Spelman, R. Stouffer, S. Manabe, and K. Bryan for providing us with the coupled ocean–atmosphere GCM data. We are also grateful to M. J. Nath and N-C. Lau for providing the high-pass filter used to obtain the storm tracks. Finally, we wish to thank J. Meehl and N. Hall for useful discussions concerning the results and intermodel comparisons.

REFERENCES

Bates, G. T., and G. A. Meehl, 1986: The effect of CO_2 concentration on the frequency of blocking in a general circulation model coupled to a simple mixed layer ocean model. *Mon. Wea. Rev.*, **114**, 687–701.

Blackmon, M. L., 1976: A climatological spectral study of the 500 mb geopotential height of the Northern Hemisphere. *J. Atmos. Sci.*, **33**, 1607–1623.

——, J. M. Wallace, N-C. Lau, and S. L. Mullen, 1977: An observational study of the Northern Hemisphere wintertime circulation. *J. Atmos. Sci.*, **34**, 1040–1053.

Bryan, K., and L. J. Lewis, 1979: A water mass model of the world ocean. *J. Geophys. Res.*, **84**(C5), 2503–2517.

Chervin, R. M., and S. H. Schneider, 1976: On determining the statistical significance of climate experiments with general circulation models. *J. Atmos. Sci.*, **33**, 405–411.

Gordon, C. T., and W. Stern, 1982: A description of the GFDL global spectral model. *Mon. Wea. Rev.*, **110**, 625–644.

Hall, N., P. Valdes, and B. Hoskins, 1992: Storm tracks in a high resolution GCM with doubled CO_2. *Quart. J. Roy. Meteor. Soc.*, submitted.

Held, I. M., 1983: Stationary and quasi-stationary eddies in the extratropical troposphere: Theory. *Large-Scale Dynamical Processes in the Atmosphere*, B. J. Hoskins and R. P. Pearce, Eds., Academic Press, 127–168.

——, and M. F. Ting, 1990: Orographic versus thermal forcing of stationary waves: The importance of the mean low-level wind. *J. Atmos. Sci.*, **47**, 495–500.

Ingram, W. J., Wilson, C. A., and J. F. B. Mitchell, 1989: Modeling climate change: An assessment of sea ice and surface albedo feedbacks. *J. Geophys. Res.*, **94,** 8609–8622.

IPCC, 1990: Scientific assessment of climate change. Intergovernmental Panel on Climate Change, J. T. Houghton, G. J. Jenkins, and J. J. Ephraums, Eds., WMO-UNEP, Cambridge University Press, 365 pp.

Kok, C. J., J. D. Opsteegh, and H. M. van den Dool, 1987: Linear models: Useful tools to analyze GCM results. *Mon. Wea. Rev.*, **115,** 1996–2008.

Lanzante, J. R., 1991: A comparison of the stationary wave responses in several GFDL increased CO_2 GCM experiments. *Proc. 16th Annual Climate Diagnostics Workshop,* Lake Arrowhead, Climate Analysis Center, National Meteorological Center, 451 pp.

Manabe, S., R. J. Stouffer, M. J. Spelman, and K. Bryan, 1991: Transient responses of a coupled ocean–atmosphere model to gradual changes of atmospheric CO_2. Part 1: Annual Mean Response. *J. Climate,* **4,** 785–818.

——, M. J. Spelman, and R. J. Stouffer, 1992: Transient responses of a coupled ocean–atmosphere model to gradual changes of atmospheric CO_2. Part 2: Seasonal response. *J. Climate,* **5,** 105–126.

Meehl, G. A., G. W. Branstator, and W. M. Washington, 1993: Tropical Pacific interannual variability and CO_2 climate change. *J. Climate,* **6,** 42–63.

Nigam, S., I. M. Held, and S. W. Lyons, 1986a: Linear simulation of the stationary eddies in a general circulation model. Part 1: The no-mountain model. *J. Atmos. Sci.*, **43,** 2944–2961.

——, ——, ——, 1986b: Linear simulation of the stationary eddies in a general circulation model. Part 2: The "mountain model." *J. Atmos. Sci.*, **45,** 1433–1452.

Schubert, S., C.-K. Park, W. Higgins, S. Moorthi, and M. Suarez, 1990: An atlas of ECMWF analyses (1980–87). NASA Tech. Memo. 100747, 273 pp. [Available from NASA, Goddard Space Flight Center, Greenbelt, Maryland.]

Siegmund, P. C., 1990a: Linear simulation of the stationary eddy response of a general circulation model to a doubling of atmospheric CO_2. Rep. DM-90-02, KNMI, 33 pp. [Available from KNMI P.O. Box 201, 3730AE De Bilt, the Netherlands.]

——, 1990b: The effect of doubling of atmospheric CO_2 on the stormtracks in the climate of a general circulation model. Rep. DM-90-02, KNMI, 12 pp. [Available from P.O. Box 201, 3730AE De Bilt, the Netherlands.]

Stouffer, R. J., S. Manabe, and K. Bryan, 1989: Interhemispheric asymmetry in climate response to a gradual increase of atmospheric CO_2. *Nature,* **342,** 660–662.

Ting, M. F., and I. M. Held, 1990: The stationary wave response to a tropical SST anomaly in an idealized GCM. *J. Atmos. Sci.*, **47,** 2546–2566.

Washington, W. M., and G. A. Meehl, 1989: Climate sensitivity due to increased CO_2: Experiments with a coupled atmosphere and ocean general circulation model. *Climate Dyn.*, **4,** 1–38.

Wilson, C. A., and J. F. B. Mitchell, 1987: A doubled CO_2 climate sensitivity experiment with a global climate model including a simple ocean. *J. Geophys. Res.*, **92,** 13 315–13 343.